FINITE ELEMENT MODEL FOR A NOVEL DEMOUNTABLE SHEAR CONNECTOR FOR STEEL-CONCRETE COMPOSITE BRIDGES

Eirini Tzouka, University of Southampton, (+44) 07546738952, E.Tzouka@soton.ac.uk
Sheida Afshan, University of Southampton, (+44) 0238059 3947, S.Afshan@soton.ac.uk
Mehdi M. Kashani, University of Southampton, (+44) 0238059 8873, Mehdi.Kashani@soton.ac.uk
Theodore L .Karavasilis, University of Patras, (+30) 2610997725, karavasilis@upatras.gr

INTRODUCTION

A three-dimensional finite element (FE) model is developed to investigate the behavior of a novel demountable shear connector for precast steel-concrete composite bridges. The connector uses high-strength steel bolts, which are fastened to the steel beam with the aid of a special locking nut configuration that prevents the slip of the bolts within their holes. The connector allows bridge disassembly and offers high level of prefabrication. In terms of sustainability, the novel shear connector facilitates the replacement of deteriorating bridge components and therefore extend the bridge design life. The accuracy of the proposed FE model is validated by comparing its results with experimental results available in the literature. Parametric studies are performed to evaluate the effects of significant parameters on the behavior and the capacity of the shear connector.

FINITE ELEMENT MODELS

Development of the FE models

Details of the geometry of the push out specimens, used in the FE Analysis, are shown in Figure 1. Because of the symmetry of the specimens, only one quarter of the push-out test arrangement was modeled. Eight-node linear hexahedral solid elements with reduced integration and hourglass control (C3D8R) were used to model all the parts of the shear connector, except from the reinforcing bars, which were meshed using two-node linear three dimensional truss elements. For computational efficiency,a coarse mesh was adopted for the overall push-out specimen, with a fine mesh being used for the region around the shear connector.

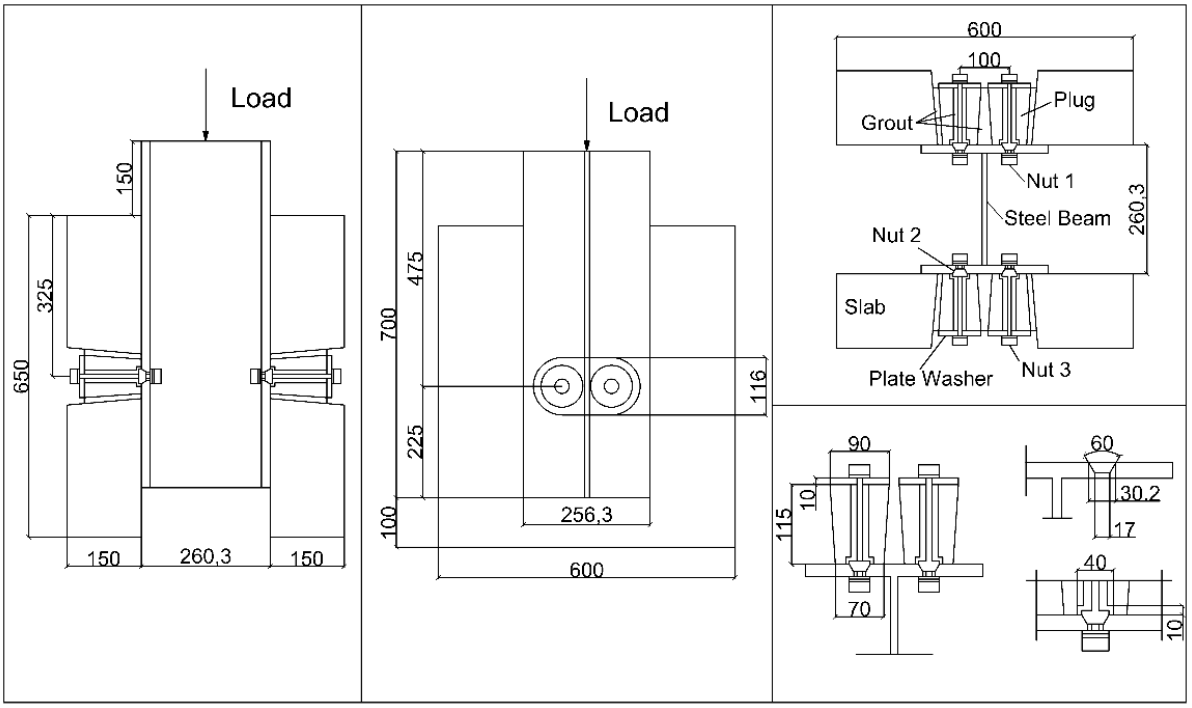

Figure 1. Details of the push-out test specimens

The surface-to-surface contact interaction was used to model the interactions between the various components of the LNSC connectors. 'Hard' and 'Penalty' options were used to describe the normal and tangential behavior between the contact surfaces, respectively. The embedded constraint option was applied to the reinforcing bars and concrete slab, in order to constrain the translational degrees of freedom (DOF) of the nodes on the rebar elements to the interpolated values of the corresponding DOF of the concrete elements. The boundary conditions used in the FE analysis represent the actual restrains of the specimens. For the quarter models, two planes of symmetry were taken into consideration, while all nodes at the bottom end of the concrete slab were restrained against all degrees of freedom.

Material Properties

A plastic model with von Mises yield function, associated plastic flow and isotropic hardening was used to model the steel beam. The bilinear plus nonlinear model proposed by Yun et al. (2) was used to describe the material behavior. For the reinforcing bars, a simpler elastic-perfectly plastic model, without strain hardening and yield strength equal to 500MPa was employed.

The stress-strain relationship of high strength bolts was defined using the material property data obtained from standard tensile tests conducting by Suwaed et al. (1). Standard tensile test models were built in Abaqus software in order to evaluate the behavior of high strength bolts. Damage initiation criteria and damage evolution models were employed in the analysis to take into account the degradation of the material stiffness and capture the stain localization in the neck region of the specimens.

Concrete Damage Plasticity (CDP) model was used to simulate the behavior of concrete materials; plugs, slabs and grout. The uniaxial stress-strain relationship proposed by Carreira & Chu (3) was used for concrete slabs and grout in compression, while plug's material properties were defined using the modified uniaxial stress-strain relationship for high strength concrete proposed by Hsu & Hsu (4). Hillerborg's fracture energy theory (5) was adopted for the tensile behavior of concrete parts, in order to minimize the mesh sensitivity of the results.

To take into account the complex nature of passively confined concrete, key material parameters were included. The ratio of the compressive strength under biaxial loading to uniaxial compressive strength (f_{b0}/f_c') was determined using the research findings of Papanikolaou and Kappos (6). The ratio of the second stress invariant on the tensile meridian to that on the compressive meridian (K_c), was expressed as a function of the compressive strength of concrete by using the equation proposed by Yu et al. (7). A value of 0.1 was adopted for the flow potential eccentricity, according to Abaqus user manual recommendations. Dilation angle values for grout, slab and plugs, were iteratively calibrated to match push-out tests results.

Analysis Procedure

A quasi-static analysis was performed by using ABAQUS/Explicit solver to allow for the use of damage and failure models with element deletion. The mass of the model was increased artificially by using the mass scaling option with time increment of 0.00001 sec for computational efficiency. Both kinetic and internal energy were monitored throughout the analysis, to ensure that the quasi-static conditions are maintained; the kinetic energy was less than 5% of the internal energy. The loading of the specimens was defined in two steps, corresponding to the experimental testing. For the first step, the pre-tensioning of the bolts was simulated by using the predefined temperature field option. On the second step of the analysis, a displacement load was applied on the upper edge of the beam flange.

Validation of numerical results

The accuracy of the FE models was verified by comparing the load-slip response and the failure modes of the specimens against the experimental test results presented by Suwaed et al (1). Three specimens were used for the validation and the results are presented in Table 1. The FE model was capable to predict the three distinct stages on the load-slip behavior of the LNSC connector. In the first stage, the shear load was approximately equal to 50% of the shear resistance, while in the second stage, the shear load increased further up to 75% of the shear resistance. In this stage, gradual yield of bolts was noticed, along with crushing of the grout in front of the conical nut and bolt shank. In the last stage, the shear load reached its ultimate value with the conical nut and the bolt shank started to bear against the concrete plug. As a result, the concrete shear strains in the part of the plug that is in front of the conical nut were increased and a concrete shear failure plane formed that passed through the grout–plug-slab surface.

Table 1. Validation of the numerical results

Test number	Bolt Diameter (mm)	Plug Compressive Strength (MPa)	Shear Resistance (kN)	Shear Resistance Ratio ($f_{u,exp}/(f_{u,FE}$)
8	14	95	148.5	1.04
10	16	50	179.6	1.00
12	16	91	186.79	1.01

Parametric study

The effects of variations in the bolt pretension and the compressive strength of grout, on the shear resistance and the load-slip behavior of the connection were assessed by carrying out parametric studies and the results are presented in Table 2. The parametric results showed that the maximum shear resistance is not considerably affected by a change in the bolt pretension (the maximum shear resistance increase was less than 4%). On the contrary, the stiffness at 50% of the shear load of the specimens is significantly increased with increasing bolt pretension.

By increasing the compressive strength of the grout, the material becomes more brittle and therefore the degradation of grout with higher strength is more rapid compared to grout with low strength. Both shear resistance and stiffness of the connector were affected from a variation in grout's compressive strength. More specifically, an increase in grout compressive strength from 20MPa to 40MPa, caused a 10% decrease in shear resistance and 15% decrease of the stiffness of the specimen.

Table 2. Validation of the FE model and parametric study results

Effect of bolt pretension					
Group	Bolt pretension (kN)	Shear Resistance (kN)	Shear Resistance Ratio ($f_{u,Pi}/(f_{u,P1}$)	Stiffness (kN/mm)	Stiffness ratio ($k_{u,Pi}/(k_{u,P1}$)
P1	26	186.79	1.00	103.03	1.00
P2	40	190.98	1.02	108.19	1.05
P3	60	190.99	1.02	115.70	1.12
P4	80	194.38	1.04	119.33	1.16
Effect of grout compressive strength					
Group	Grout Compressive Strength (MPa)	Shear Resistance (kN)	Shear Resistance Ratio ($f_{u,Gi}/(f_{u,G1}$)	Stiffness (kN/mm)	Stiffness ratio ($k_{u,Gi}/(k_{u,G1}$)
G1	20	190.47	1.00	101.76	1.00
G2	28	186.79	0.98	103.03	1.01
G3	32	180.179	0.95	100.80	0.99
G4	40	171.299	0.90	85.63	0.84

REFERENCES

(1) Suwaed ASH, Karavasilis LT, Novel Demountable Shear Connector for Accelerated Disassembly, Repair, or Replacement of Precast Steel-Concrete Composite Bridges. Journal of Bridge Engineering, 2017;22(9):04017052.

(2) Yun X, Gardner L, Stress-strain curves for hot-rolled steels. Journal of Constructional Steel Research, 2017;133:(36-46).

(3) Carreira D, Chu K, Stress–strain relationship for plain concrete in compression. ACI Journal, 1985; 82:(797-804).

(4) Hsu L, Hsu C, Complete stress - strain behavior of high-strength concrete under compression. Magazine of Concrete Research, 1994;169:(301-312).

(5) Hillerborg A, Modéer M, Petersson PE, Analysis of crack formation and crack growth in concrete by means of fracture mechanics and finite elements. Cement and Concrete Research, 1976;6(6):(773-781).

(6) Papanikolaou V, Kappos A, Confinement-sensitive plasticity constitutive model for concrete in triaxial compression. International Journal of Solids and Structures, 2007;44:(7021–7048).

(7) Yu T, Teng JG, Wong YL, Dong SL, Finite element modeling of confined concrete-I: Drucker–Prager type plasticity model. Engineering Structures, 2010;32(3):(665-679).